

## Investigation of Black-Gray Soliton Interaction

Dmitri Foursa\* and Philippe Emplit

*Université Libre de Bruxelles, Service d'Optique et d'Acoustique, 50 Avenue F. Roosevelt, CP 194/5, B-1050 Bruxelles, Belgium*

(Received 1 July 1996)

We demonstrate the first experimental investigation of the interaction between black and gray solitons in an optical fiber. The fiber length equals 8 soliton distances. The repulsive character of the interaction is observed during the walk-off of the gray soliton through the black one inside the finite-width background carrier pulse. Opposite cases of the gray soliton phase profile are studied, corresponding to gray pulses with a group velocity higher and smaller than that of the carrier pulse. Numerical simulations presented show good agreement with experimental data. [S0031-9007(96)01610-9]

PACS numbers: 42.81.Dp

The nonlinear Schrödinger equation (NSE) predicts the existence of stable solutions, conserving amplitude, and phase under propagation, for both positive and negative group velocity dispersion (GVD) regions. The solution existing in the positive GVD region is a rapid intensity dip in a cw background and is called a “dark” soliton analogously to the so called “bright” soliton for the negative GVD region [1,2]. The particular case of the dark soliton and the most studied one is the pulse, which is an antisymmetric function of time with an abrupt  $\pi$  phase shift and zero intensity at its center and will be referred to as a “black” soliton in the following.

However, the intensity of the dark soliton does not generally dip all the way to zero. This type of pulse is called a gray soliton and the contrast of the dip, defined by Tomlinson *et al.* [3], is determined by the blackness parameter  $|B| < 1$  (pulses with  $|B| = 1$  correspond to black solitons). Gray solitons have a phase profile which is also an antisymmetric function of time, but with a smaller and more gradual phase shift than that of black solitons. For gray solitons the time-dependent phase shift represents an effective frequency shift, and therefore gray pulses propagate at velocities different from the group velocity of the background. It will advance with respect to the background for  $B < 0$  and lag behind it for  $B > 0$ . The rate at which gray solitons walk off from the background increases with decreasing blackness [4].

Dark soliton properties have been investigated extensively over the last few years due to their potential application as carrier bits in telecommunication systems [3,5–16]. Several techniques have been proposed to generate isolated odd-symmetry black pulses [3,5,6], or CW trains of black solitons [9,11–15]. Thurston *et al.* demonstrated the generation of single gray solitons on a finite duration background [8].

Already in early investigations by Blow and Doran [16], it was shown that dark solitons interact repulsively and that an even-symmetry dark pulse breaks up into two gray solitons with identical amplitude but opposite signs of  $B$ . The evolution of even-symmetry dark pulse into two complementary gray solitons was later experimentally

verified [17]. It was also shown that an odd-symmetry dark pulse at powers, exceeding the power of a fundamental soliton, emits a pair of symmetrical gray solitons [18].

Optical spatial solitons, which are solutions of the two-dimensional spatial NSE with defocusing nonlinearity, exhibit properties similar to those of temporal solitons in optical fibers [19]. As in the case of temporal solitons, simulations of multiple spatial soliton propagation demonstrated that they interact repulsively [20].

To date, due to the absence of shaping techniques, enabling one to generate a couple of dark pulses with different phase profiles and different signs of  $B$ , interaction of black and gray solitons in optical fibers has been studied only theoretically [8,16,21], to our knowledge.

In this Letter we report the first experimental investigation of black-gray soliton pair behavior. Two dark pulses with controlled phase profiles are shaped on a relatively large but finite-width background carrier pulse. A number of previously published works revealed that, under such conditions, propagational properties of dark pulses are similar to those of the solitons on the infinite background [3,5–8,21].

*Experimental results.*—The odd-symmetry dark pulses are produced in a shaping setup based on the space-to-time transformation properties of a spectrographlike arrangement [10]. The input for the shaping setup is nearly transform limited 1.8 ps pulses (FWHM intensity assuming  $\text{sech}^2$  shape) emitted at an 82 MHz repetition rate by a mode-locked Ti:sapphire laser (Fig. 1). The central wavelength of these pulses is fixed at 886.5 nm. Their duration is monitored by a scanning intensity autocorrelator. With the phase plate producing the  $\pi$  phase shift, the shaping setup delivers 3 ps (FWHM) odd-symmetry black pulses located on a 37 ps (FWHM) background. In addition to the  $\pi$  phase plate, a second phase plate is added. By choosing the value of the phase shift imposed by the latter one, gray pulses with any blackness parameters could be generated on the same carrier pulse. The sign of the blackness parameter  $B$  can be altered by the rotation of the second wave plate by  $180^\circ$  around the beam axis. Both wave plates are

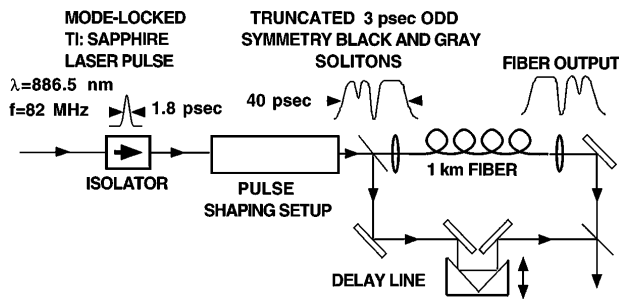


FIG. 1. Experimental setup.

fixed on two independent translation and rotation stages to allow the precise adjustment of the phase and timing of the black and gray solitons inside the background carrier. The shaping setup delivers up to 10 mW of signal average power when pumped by 1.2 W.

Experiments are carried out with the use of 1 km single-mode fiber with an effective core area of  $28 \mu\text{m}^2$  and dispersion of 90 ps/nm/km. The fiber length equals approximately 8 soliton distances. The coupled signal power exceeds (approximately by 25%) the level of the fundamental dark soliton in order to partially compensate for the fiber losses.

Temporal and spectral measurements of shaping and fiber output signals are performed, respectively, by a streak camera and a grating spectrograph [10]. The impulse response of the streak camera is 6.7 ps (FWHM). Although not giving the possibility to resolve the pulse shape under investigation, it still is sufficient to study the temporal position and the qualitative behavior of generated solitons [5,7]. For instance, the broadening or the compression of dark pulses corresponds to the increase or the decrease of the contrast of the streak camera image of pulses. Parts of the radiation from the shaping setup and the fiber output are synchronized and simultaneously directed to the streak camera to enable the observation of both signals at the same time. The spectrum is monitored by a grating spectrograph with the resolution of  $1.8 \times 10^{-2} \text{ nm}$ , i.e., 7.5 GHz.

As predicted by Thurston *et al.* [8], the evidence of the interaction taking place during the propagation is a change of the arrival time for both dark pulses with respect to the interaction-free case. In order to observe the effect, we first propagate both pulses in a way the gray pulse, initially well separated from the black one, will completely walk through the black soliton and could be clearly resolved at the fiber output. This is achieved by adapting the original position of the gray pulse to its blackness sign and by the adjustment of its global phase shift. The total phase shift of the gray pulse was found to be  $0.68\pi$ , corresponding to  $|B| = 0.88$ . The background peak power coupled into the fiber is adjusted to approximately 2 W, which slightly exceeds the power of the fundamental soliton (1.6 W).

In a second step, without changing any adjustments, we propagate only a single black pulse with  $\pi$  phase shift to

record its exact position on the carrier pulse at the input and output of the fiber.

Finally, in a similar way, we propagate only the gray pulse on the background. Comparing the three sets of measurements, we estimate the shift induced by the interaction forces.

The streak camera image shown in Fig. 2(a) displays the temporal profiles of the shaping output (left curve) and the fiber output (right curve) of a single gray pulse. During the propagation in the fiber, the gray soliton with  $B > 0$  clearly walks off from the leading ( $-10$  ps) to the trailing part ( $+4$  ps) of the carrier pulse. The asymmetry of the gray pulse's profile is due to the limited streak camera resolution. At the same time the carrier pulse disperses in time because of the dispersion and self-phase modulation effects. Dark and gray solitons are also becoming broader after the propagation in the fiber due to the fiber losses and the decrease of the carrier pulse amplitude.

In order to have the initial positioning of dark soliton pulses for reference, a temporal measurement has been performed with only the single  $\pi$  phase plate for the black pulse generation installed in the shaping setup [Fig. 2(b)].

The temporal measurement, when both dark and gray solitons were formed at the same time, revealed the following behavior of the pulses [Fig. 2(c)]. When placed on the leading part of the carrier pulse, gray soliton shifts its position after propagation in the fiber (dotted cursor) and walks through the dark pulse (solid cursor). As a result of the interaction with the dark soliton, gray pulse walk-off increases by 3 ps [compared Figs. 2(a) and 2(c)]. At the same time dark pulse also changes its position towards the leading edge of the carrier pulse by 2 ps [see Figs. 2(b) and 2(c)].

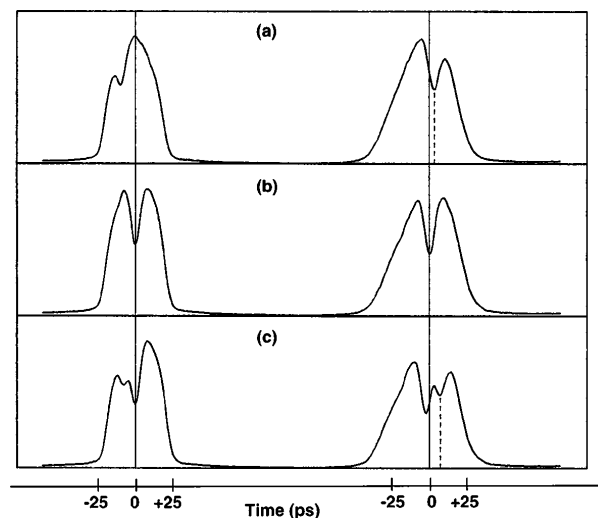


FIG. 2. Streak camera images of the pulses at the shaping output (left curves) and at the fiber output (right curves) for  $B = 0.78$ . (a) Single gray pulse, (b) single black pulse, and (c) gray and black pulse pair. Black solitons are marked by solid cursors and gray pulses at the fiber output by dotted lines.

We have also performed the investigation of the black and gray soliton interaction with the blackness parameter of the latter ones  $B < 0$  and the same equivalent global phase shift. Results are depicted in Fig. 3. The timings are found to be consistent with the case of  $B > 0$ .

The reason that our investigation is limited to one absolute value of the parameter  $|B|$  only is connected with two factors. For greater values of  $|B|$  the length of the fiber available was not sufficient for the gray soliton to completely walk through the black one. Whereas for the smaller values of  $|B|$  the contrast of the dip decreases, which makes it difficult to observe the pulses with already limited resolution of the streak camera.

*Numerical simulations.*—It has been shown that for the positive GVD wavelength region of optical fibers, pulses of the form

$$U(t) = (A_0/|B|) \times [1 - B^2 \text{sech}^2(A_0 t/t_0)]^{1/2} \exp[i\varphi(A_0 t/t_0)], \quad (1)$$

$$\varphi(\xi) \equiv \sin^{-1} \left[ \frac{-B \tanh(\xi)}{(1 - B^2 \text{sech}^2(\xi))^{1/2}} \right] \quad (2)$$

are soliton solutions of NSE for the blackness parameter  $|B| \leq 1$  [3]. For the limiting case of  $|B| = 1$  the above equations reduce to

$$U(t) = A_0 \tanh(A_0 t/t_0), \quad (3)$$

which represents a black soliton [2].

The normalized peak intensity of both black and gray solitons is given by  $I = |A|^2$ . The full width at half peak (the depth) of the intensity is  $\tau = 1.76/|A|$  (in units of  $t/t_0$ ). The total phase shift across a gray soliton is  $2 \sin^{-1}|B|$  [3].

To solve the pulse propagation problem we use the split-step Fourier method [22].

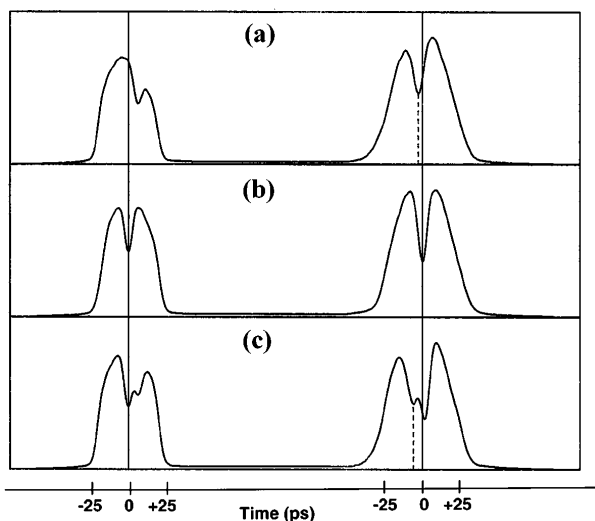


FIG. 3. Streak camera images for  $B = -0.78$  of the shaping output (left curves) and the fiber output (right curves). (a) Single gray pulse, (b) single black pulse, and (c) gray and black pulse pair.

In the present investigation we consider 3 ps (FWHM) gray and black solitons with the form given by (1)–(3), superimposed on the carrier pulse  $U(t) = A \text{sech}[-(t/12t_0)^2]$  with the FWHM of 38 ps. Parameters of the fiber are taken the same as used in experiment. Results of numerical simulations for  $B = 0.77$  and an input black pulse amplitude  $A = 1.25$  are presented in Figs. 4(a) and 4(b) and show that after propagation in the fiber, dark solitons are retaining their initial shape, although broadening to some extent. The carrier pulse also becomes broader because of normal dispersion and self-phase modulation effects, which apart from the fiber attenuation contribute to the decrease of its amplitude. The gray soliton, initially located on the leading part of the carrier pulse [Fig. 4(a)], moves to later times during propagation in the fiber and crosses the black soliton completely [Fig. 4(b)]. As a result of the interaction, the black soliton shifts toward earlier times from its central position by approximately 2 ps.

Figures 4(c) and 4(d) show the input and output of the fiber with only gray soliton located on the carrier pulse at the same initial position, as in Fig. 4(a). Comparing Figs. 4(a) and 4(b) and Figs. 4(c) and 4(d), one can see that the overall walk-off of the gray soliton during the propagation in the fiber increases from 13.5 ps (with no interaction) to 16.5 ps after crossing the black soliton.

Numerical simulations carried out for the negative value of  $B = -0.77$  display the opposite situation. Simulations are also performed for the case of the dark solitons placed on the CW background and revealed the same basic behavior of pulses as in the case of the finite carrier pulse.

In conclusion, the first experimental evidence of the black-gray soliton interaction in an optical fiber has been

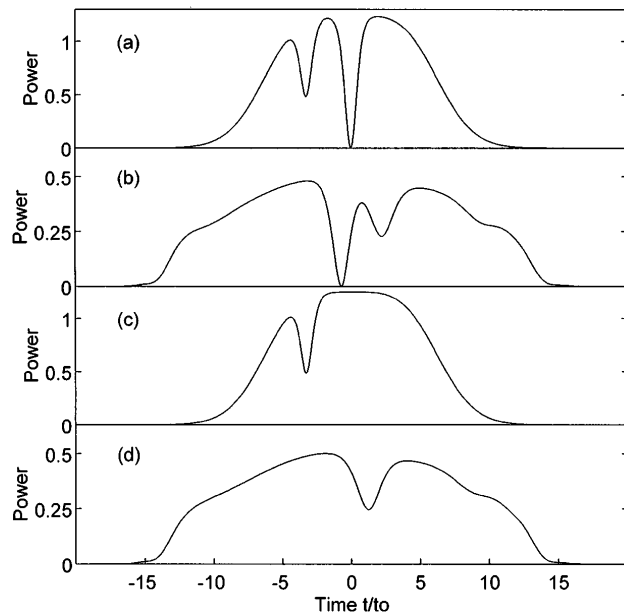


FIG. 4. Numerical simulation for  $B = 0.77$ . Temporal profiles of the black and gray pair at the fiber input (a) and output (b). Single gray soliton at the fiber input (c) and output (d).

demonstrated. The observed behavior of the black and gray solitons after the collision leads to the conclusion that the interaction of the dark-gray soliton pair has a repulsive character when a complete walk-off of the gray soliton through the dark one is taking place for both cases of blackness parameters  $B < 0$  and  $B > 0$ . That means that the faster soliton arrives earlier and the slower one arrives later if they pass through each other. As was apparent after the investigation, the gray soliton time shift, brought on by the interaction, is higher than that of the black soliton (particularly 1.5 times higher for  $|B| = 0.78$ ). The delay times in arrival of dark solitons after propagation in the fiber are found to be approximately equal for  $B > 0$  and  $B < 0$ . The collision induced time shifts are in consistency with general prediction of previous theoretical papers [8,16].

Numerical simulations performed show good agreement with experimental results. We found that propagational timing properties of dark solitons on the finite carrier pulse are similar to those of the dark pulses on CW background. Although temporal timings resulting from the interaction between black and gray solitons are well defined, the interpretation of the spectral images is more complicated and needs further investigation.

Dmitri Foursa acknowledges the Belgian OSTC for providing him a postdoctoral fellowship. This research was supported by Interuniversity Attraction Poles program of the Belgian OSTC under Grant No. P3-047.

---

\*Permanent address: Fiber Optics Research Centre (FORC) at General Physics Institute, Russian Academy of Sciences, 38 Vavilov Strasse, 117942 Moscow, Russia.

- [1] V.E. Zakharov and A.B. Shabat, *Sov. Phys. JETP* **5**, 364 (1972).
- [2] A. Hasegawa and F. Tappert, *Appl. Phys. Lett.* **23**, 171 (1973).
- [3] W.J. Tomlinson, R.J. Hawkins, A.M. Weiner, J.P. Heritage, and R.N. Thurston, *J. Opt. Soc. Am. B* **6**, 329 (1989).
- [4] A.M. Weiner, in *Optical Solitons-Theory and Experiment*, edited by J.R. Taylor (Cambridge University Press, Cambridge, England, 1992).
- [5] Ph. Emplit, J.-P. Hamaide, F. Reynaud, C. Froehly, and A. Barthélémy, *Opt. Commun.* **62**, 374 (1987).
- [6] A.M. Weiner, J.P. Heritage, R.J. Hawkins, R.N. Thurston, E.M. Kirschner, D.E. Leaird, and W.J. Tomlinson, *Phys. Rev. Lett.* **61**, 2445 (1988).
- [7] Ph. Emplit, M. Haelterman, and J.-P. Hamaide, *Opt. Lett.* **18**, 1047 (1993).
- [8] R.N. Thurston and Andrew M. Weiner, *J. Opt. Soc. Am. B* **8**, 471 (1991).
- [9] W. Zhao and E. Bourkoff, *J. Opt. Soc. Am. B* **9**, 1134 (1992).
- [10] Ph. Emplit, J.-P. Hamaide, and F. Reynaud, *Opt. Lett.* **17**, 1358 (1992).
- [11] A.V. Shipulin, D.G. Fursa, and E.A. Golovchenko, *Sov. Lightwave Commun.* **3**, 153 (1993).
- [12] D.J. Richardson, R.P. Chamberlin, L. Dong, and D.N. Payne, *Electron. Lett.* **30**, 1326 (1994).
- [13] M. Nakazawa and K. Suzuki, *Electron. Lett.* **31**, 1076 (1995).
- [14] M. Haelterman and Ph. Emplit, *Electron. Lett.* **29**, 356 (1993).
- [15] R. Leners, D. Foursa, Ph. Emplit, M. Haelterman, and R. Kashyap, in *Technical Digest of European Conference on Lasers and Electro-Optics/European Quantum Electronics Conference*, Hamberg, Germany, 1996 (No. CTuJ4, p. 87).
- [16] K.J. Blow and N.J. Doran, *Phys. Lett.* **107A**, 55 (1985).
- [17] D. Krokkel, N.J. Halas, G. Giuliani, and D. Grischkowsky, *Phys. Rev. Lett.* **60**, 29 (1988).
- [18] A.M. Weiner, J.P. Heritage, R.J. Hawkins, R.N. Thurston, E.M. Kirschner, D.E. Leaird, and W.J. Tomlinson, *Phys. Rev. Lett.* **61**, 2445 (1988).
- [19] Yuri S. Kivshar, *IEEE J. Quantum Electron.* **29**, 250 (1993).
- [20] B. Luther-Davies and Xiaoping Yang, *Opt. Lett.* **17**, 1755 (1992).
- [21] G.L. Diankov and I.M. Uzunov, *Opt. Commun.* **117**, 424 (1995).
- [22] Govind P. Agrawal, *Nonlinear Fiber Optics* (Academic Press, New York, 1995).